

# Efficiency of Particle Entrapment by Single Bubble

Yuichi TSUKAGUCHI\*

## Abstract

*Bubbles are commonly used to remove inclusions in steel refining and steel casting processes. However, the mechanism is unclear because multiple phenomena are involved complicatedly in the inclusion capturing or the inclusion transfer process by bubbles. Therefore, we undertook research work to clarify the efficiency of inclusion capturing by a single bubble. Such work was conducted by a water model experiment that blows bubbles into the swirl flow of water in which particles are suspended. As a result, the capture efficiency of non-wettable particles coincided with the estimated value of the Sutherland model or Weber & Paddock model. However, wettable particles were not captured by a single bubble.*

## 1. Introduction

Bubbles are commonly used to remove nonmetallic inclusions in steel refining and steel casting processes. However, the mechanism is unclear because multiple phenomena are involved complicatedly. Such phenomena include direct capturing of particles by bubbles, inclusion transfer by vortices below bubbles, and inclusion transfer by ascending flows generated by bubbles. Therefore, Nippon Steel Corporation conducted research to clarify the efficiency of inclusion capturing by a single bubble, which is the most basic phenomenon in inclusion removal by bubbles. This study used a water model experimental apparatus to obtain the capturing efficiency by a single bubble.

## 2. Main Issue

### 2.1 Outline

To obtain the capturing efficiency of particles by a single bubble, bubbles are blown into a cylinder filled with particle dispersed water. The sweep volume of the bubbles is calculated from the number of bubbles and their trajectories. Changes in the concentration of the particles are also measured. If bubbles wobble while floating to the surface or their trajectories are in a spiral, calculation of the sweep volume becomes difficult. Therefore, in this study, bubbles were blown into the swirl flow to reduce fluctuation of the bubble trajectories in order to facilitate estimation of the sweep volume.

### 2.2 Experimental apparatus

Figure 1 outlines the water model experimental apparatus. The acrylic main cylinder (cylindrical container) was placed in an acrylic square case and placed on a magnetic stirrer. A SUS air nozzle with an inner diameter of 0.51 mm was installed onto the side wall (150

mm from the bottom). Bubbles blown in from the air nozzle move to the center while circling and floating by centripetal force working in the swirl flow. They pass through the collector tube to enter the collector cylinder. Particles captured by bubbles were transferred into the collector cylinder with bubbles.

The stirrer in the collector cylinder has six blades: The height of the blade is 18 mm, the thickness is 2 mm, and the diameter is 34 mm. The depth of the bath in the main cylinder is 350 mm (capacity: 1 759 mL). 200 mL of water was poured into the collector cylinder. The flow rate of the air was 60 mL/min.

The flow velocity distribution in the main cylinder in the experimental apparatus was measured in advance using a laser Doppler velocimeter. Figure 2 shows the results (the data on 600 rpm in the

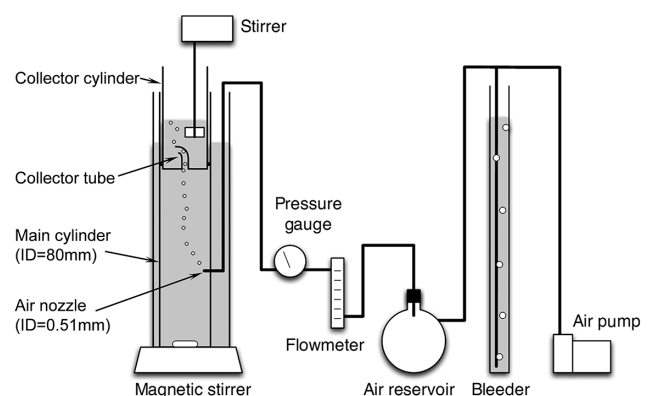


Fig. 1 Schematic view of water model experiment

\* Senior Researcher, Ph. D., Steelmaking Research Lab., Process Research Laboratories  
16-1 Sunayama, Kamisu City, Ibaraki Pref. 314-0255

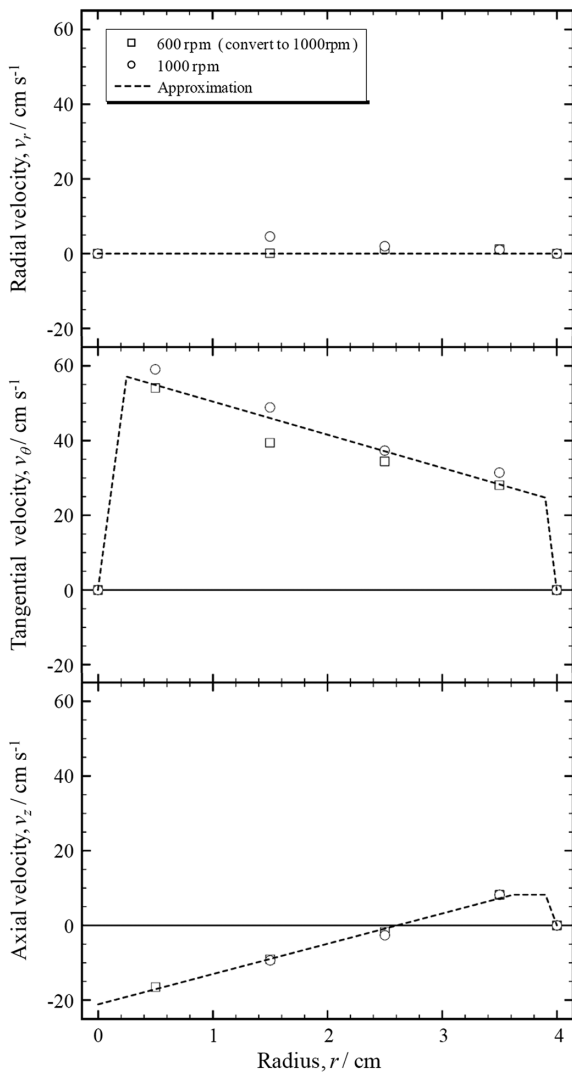


Fig. 2 Distribution of flow velocity

figure was obtained by multiplying the measured values by 10/6). Based on the results in Fig. 2, the flow velocity in the radial, circumferential, and vertical directions when the rotation speed of the magnetic stirrer was 1 000 rpm was approximated as shown in the equations below against the radius,  $r$ . It was assumed that each flow velocity would change linearly with the rotation speed of the magnetic stirrer.

$$v_r = 0$$

$$v_\theta = \begin{cases} 228.4r & (0 \leq r < 0.0025) \\ -8.871r + 0.5932 & (0.0025 \leq r < 0.039) \\ -247.2r + 9.889 & (0.039 \leq r \leq 0.04) \end{cases}$$

$$v_z = \begin{cases} 8.108r - 0.2113 & (0 \leq r < 0.036) \\ 0.08221 & (0.036 \leq r < 0.039) \\ -82.21r + 3.288 & (0.039 \leq r \leq 0.04) \end{cases}$$

### 2.3 Particles used

Table 1 lists the two types of particles suspended in the main cylinder. The polystyrene particles get wet (wetable particles) and the acrylic particles do not (non-wetable particles). The contact angles listed in Table 1 were measured by the penetration rate method. Although the contact angles differ only by 10 degrees between the two types of particles, the wettability of the two types of particles is

Table 1 Specifications of particles

Material	Density $\rho$ (kg/m <sup>3</sup> )	Contact angle $\theta$ (degree)	Shape
Polystyrene	1 130	80	Spherical
Acrylic	1 210	90	Spherical

\* Polystyrene: Soken Chemical & Engineering Co., Ltd. SGP-70,  
Acrylic: Soken Chemical & Engineering Co., Ltd. MR-20

clearly different; when particle suspensions are prepared, the polystyrene particles easily disperse, while the acrylic particles tend to condense on the beaker wall and water surface.

Figure 3 shows the distribution of the particle diameters along with a photograph of each type of particle. All the particles are white fine powder for which the model diameter is approximately 5  $\mu\text{m}$ . The particle suspension was prepared by dispersing 8.0 g of each type of particle to 500 mL of water using an ultrasonic homogenizer. The prepared particle suspension was added to the main cylinder by 20 mL or 60 mL (mainly 60 mL) for experiments. When 60 mL of the particle suspension was added, the water in the main cylinder became cloudy. Rough changes in the particle concentration were visually observed from changes in the cloudiness.

### 2.4 Experimental procedures

Particle capturing experiments were performed while bubbles were blown into the main cylinder. The experimental procedure is shown below. It was confirmed in a preliminary experiment that in a swirl flow without bubbles blown in, particles do not condense (when no bubbles are blown in, the grain size distribution does not change even when the time elapses).

1. Pure water was poured into the main cylinder to the designated depth (350 mm).
2. The particle suspension was added to the main cylinder.
3. The water in the main cylinder was stirred with the magnetic stirrer at a rotational speed of 600 or 1000 rpm for approximately one minute to disperse particles.
4. The water in the main cylinder was sampled by 1.6 g. This sample was used as the initial condition (the bubble blow-in time is zero).
5. A collector cylinder was installed onto the upper section of the main cylinder.
6. A designated amount of pure water (200 mL) was poured into the collector cylinder.
7. A stirrer was attached to the inside of the collector cylinder. The water was slowly stirred at a rotation speed of 180 rpm (to prevent the particles from sinking).
8. Blowing-in of air was started at a designated flow rate (60 mL/min). The time ( $t$ ) when the first bubble was emitted was regarded as zero and timing was started.
9. The water in the collector cylinder was sampled by 1.6 g at designated intervals (3 min) until 18 min.
10. The number of particles in the sampled water was counted using a multisizer (Multisizer3 made by Coulter Counter Ltd.)

### 2.5 Experimental results and discussion

#### 2.5.1 Results for wettable particles

In the case of wettable particles, the particle concentration in the main cylinder (calculated from the particle concentration in the collector cylinder) simply decreased as the time elapsed as shown in Fig. 4, regardless of the particle diameter and the rotation speed of the magnetic stirrer. These results show that wettable particles may

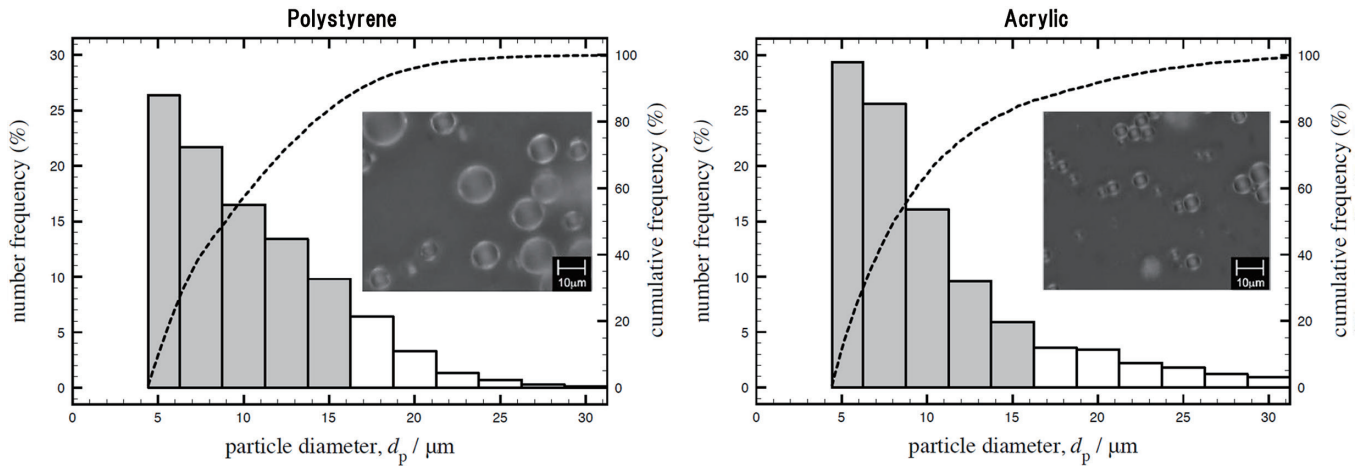


Fig. 3 Distribution of particle diameter

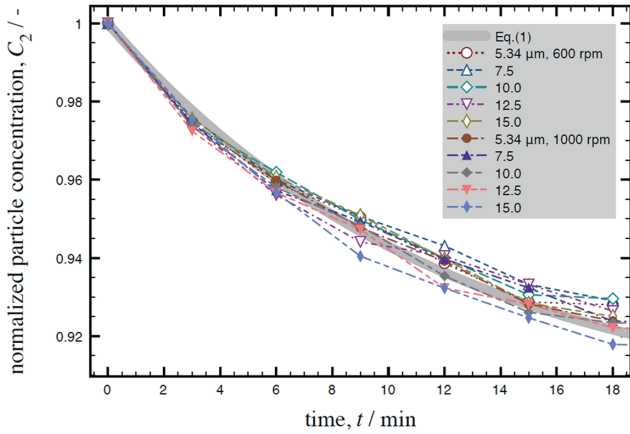


Fig. 4 Change in density of wettable particles in main cylinder

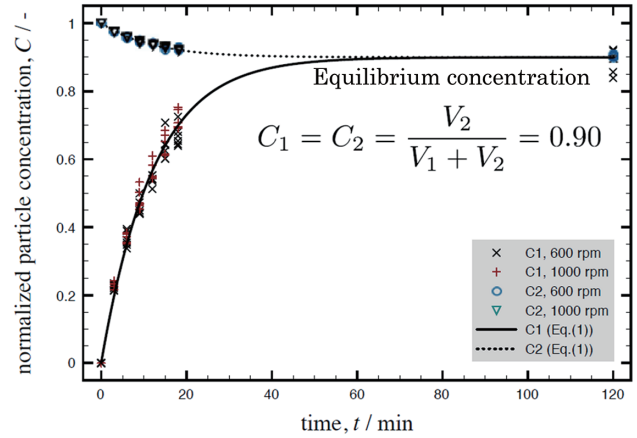


Fig. 5 Change in density of wettable particles in both cylinders

not be captured by bubbles and they may disperse due to liquid exchange caused by the bubbles traveling from the main cylinder to the collector cylinder.

Therefore, changes in the particle concentration were expressed as simple models shown below and compared with the experimental results to estimate the exchange volume,  $\Delta V$ , per unit time.

$$\frac{dC_1}{dt} = \frac{\Delta V}{V_1} (C_2 - C_1) \quad (1)-1$$

$$\frac{dC_2}{dt} = \frac{\Delta V}{V_2} (C_2 - C_1) \quad (1)-2$$

Where,  $C_1$  is the particle concentration in the collector cylinder and  $C_2$  is that in the main cylinder. When  $t$  is 0,  $C_1$  is 0 and  $C_2$  is 1.

As shown in Fig. 5, when the particles are not transferred by bubbles, the particle concentration in the collector cylinder and that in the main cylinder reach a certain equilibrium concentration that is determined by the volume ratio of the two cylinders. As a fitting parameter for the concentration change rate, the liquid change volume per unit time was obtained at 14.7 mL/min.

### 2.5.2 Results for non-wettable particles

In the case of non-wettable particles, the particle concentration in the collector cylinder became higher than that in the main cylinder as the time elapsed, as shown in Fig. 6. This indicates that the non-wettable particles attached to the bubbles and were transferred into the collector cylinder from the main cylinder.

This change in the particle concentration is expressed by Equa-

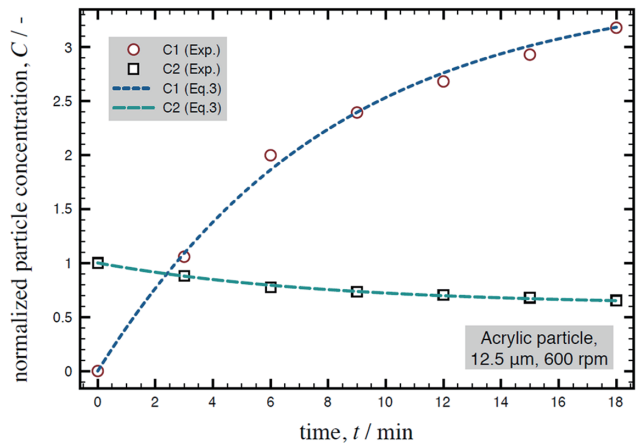


Fig. 6 Change in density of non-wettable particles in both cylinders

tions (2) and (3) by adding a term for concentration variation due to the transfer by bubbles to the aforementioned Equation (1).

$$\frac{dC_1}{dt} = \frac{\Delta V}{V_1} (C_2 - C_1) + \frac{V_2}{V_1} k_g C_2 \quad (2)$$

$$\frac{dC_2}{dt} = \frac{\Delta V}{V_2} (C_2 - C_1) - k_g C_2 \quad (3)$$

In these equations,  $C_1$  is the particle concentration in the collector

cylinder,  $C_2$  is that in the main cylinder, and  $k_g$  is a particle removal rate constant, and when  $t$  is 0,  $C_1$  is 0 and  $C_2$  is 1.

2.5.3 Particle removal rate constant

Two types of experiments were performed: Bubbles were blown in from the inner wall surface while in the other case, bubbles were blown in from the center of the main cylinder (Fig. 7). Based on the difference in the results, the number of particles was calculated that were captured by the bubbles while the bubbles traveled from the inner wall surface to the center by centripetal force.

Figure 8 shows the particle removal rate constants along with the particle diameters obtained in the experiments. The results were used to calculate the particle removal rate constant during the period in which the bubbles traveled from the side wall to the central axis region, passing through the swirl flow, by subtracting the particle removal rate constant in the central axis region from that for the entire region as expressed by Equation (4).

$$k_{g,bulk} = k_g - \alpha \cdot k_{g,axis} \quad (4)$$

Where,  $\alpha$  is the ratio of the distance in which the bubbles were swept onto the central axis in the experiment using a sidewall nozzle to that in the experiment using an L-shaped nozzle.

Figure 9 shows that the particle removal rate constants in the swirl flow region linearly increase as the particle size increases. Re-

garding the influence of the rotation speed of the magnetic stirrer, the higher the rotation speed, the smaller the particle removal rate constant. This may be because when the rotation speed of the magnetic stirrer is high, bubbles blown in from the sidewall quickly move to the central axis region and thereby the sweep distance of the bubbles is shorter.

2.5.4 Particle capture efficiency

Next, as a more common index, the particle capture efficiency was defined. The aforementioned particle removal rate constant can be expressed by Equation (5).

$$k_g = \beta_0 \cdot E \cdot C_b \quad (5)$$

Where,  $\beta_0$  is the collision rate function [ $m^3s^{-1}$ ],  $E$  is the particle capture efficiency, and  $C_b$  is the concentration of bubbles [ $m^{-3}$ ].

$\beta_0$  equals the volume that the bubbles sweep per unit time and can be expressed by Equation (6) (refer to Fig. 10).

$$\beta_0 = \frac{\pi(d_p + d_b)^2}{4} \cdot u_b \quad (6)$$

Where,  $d_p$  is the diameter of the particle,  $d_b$  is that of the bubble, and  $u_b$  is the relative velocity of the bubble against the liquid.

The bubble diameter was calculated as a sphere-equivalent diameter based on mean bubble volume that was obtained by dividing the air flow rate of 60 mL/min by the number of bubbles formed per unit time that was counted using images taken by a high-speed cam-

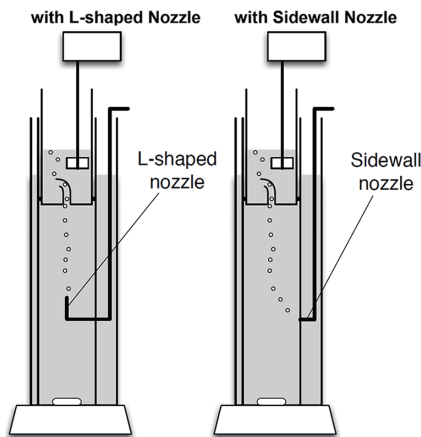


Fig. 7 Schematic view of water model experiments with two types of nozzle settings

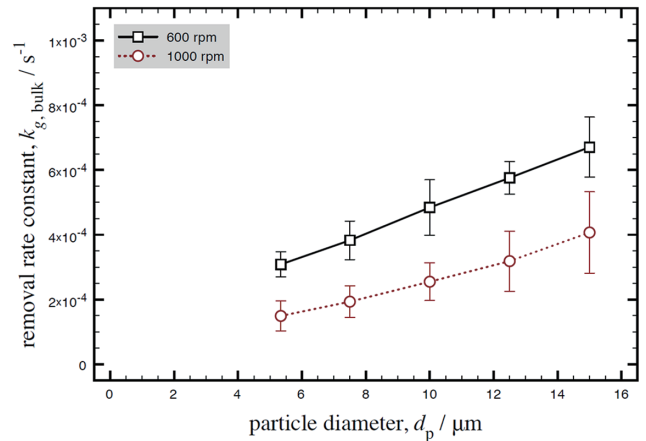


Fig. 9 Particles removal rate constant in swirl flow region

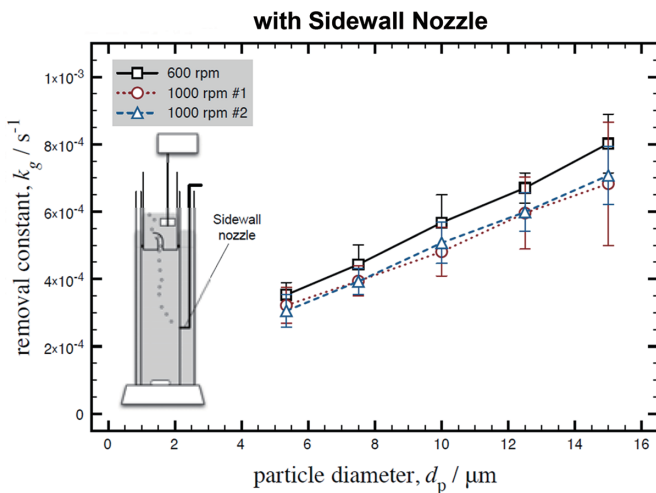
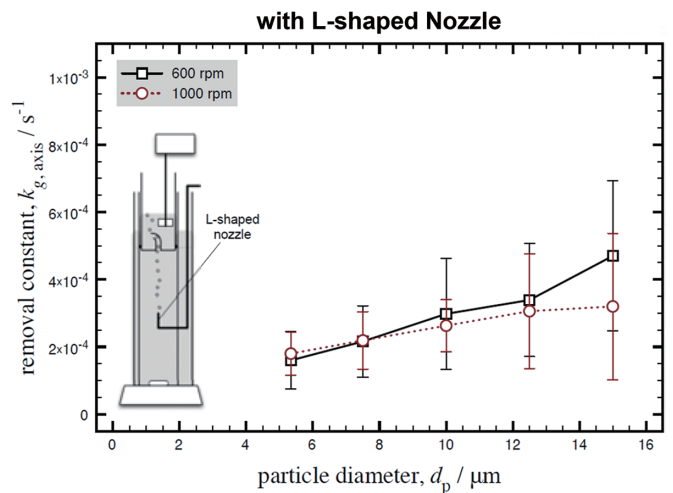


Fig. 8 Experimental results with two types of nozzle settings



era. **Table 2** lists the results. **Figure 11** shows example still images taken by the high-speed camera when bubbles were blown in from the sidewall nozzle. Figure 11 shows that the higher the rotation speed of the magnetic stirrer, the smaller the size of the bubbles and the more quickly they move to the center. The bubbles are almost spherical.

When air is blown in from the sidewall, the higher the rotation speed, the smaller the bubbles. This may be due to shear by a rotational flow and the suction by the centripetal force. On the other hand, when air is blown onto the central axis, the higher the rotation speed, the larger the bubbles. This may be because as the rotation speed is higher, the secondary downward flow at the center of the cylinder becomes strong, which reduces the floating speed of the bubbles and thereby they come closer to each other, which accelerates the coalescence of them. It has been confirmed that when air is blown in from the sidewall, bubbles that reached the central axis coalesce to become larger and the bubble diameter becomes almost

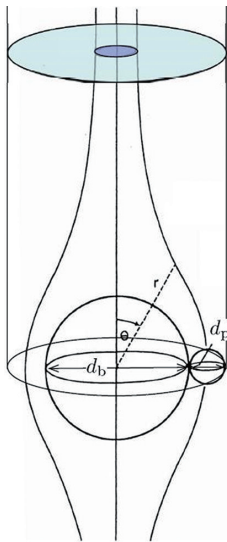


Fig. 10 Sweep volume of bubble to capture particle

equal to that of bubbles in the case where the air is blown in from the central axis.

The travel speed of the bubbles was calculated using the flow velocity data shown in Fig. 2 and Basset-Boussinesq-Oseen-Tchen (BBOT) equation.<sup>1)</sup> Data on the trajectories (time-coordinates) of the bubbles obtained from images of bubble trajectories taken by the high-speed camera (images from both of the front and the side were taken at the same time using a mirror) was compared with the results calculated by the BBOT equation and it was confirmed to almost agree with each other.

From Equation (5), the particle capture efficiency (ratio of particles that are removed to the outside of the system by bubbles to those that have come into the trajectory region of bubbles) is given by Equation (5)′.

$$E = \frac{k_g}{\beta_0 \cdot C_b} \quad (5)'$$

**Figure 12** shows the particle capture efficiency calculated using Equation (5)′ along with the particle and bubble diameters. As shown in Fig. 12, the particle capture efficiency in the swirl flow region linearly increases as the ratio of particle diameter to bubble diameter increase. That is to say, generation of small bubbles is effective to capture small particles. The differences observed in the results between the rotation speed of the magnetic stirrer of 600 rpm and that of 1000 rpm in Fig. 12 were disregarded because there were within variation of the data.

Figure 12 also shows the values calculated using capture efficiency models that were clarified in past researches. The experimental results well agree with the results calculated using the model that

Table 2 Bubble diameter blown-in from nozzles

Nozzle	Rotation speed of magnetic stirrer	Bubble diameter $d_b$
Sidewall nozzle	600 rpm	3.03 mm
	1000 rpm	2.57 mm
L-shaped nozzle	600 rpm	4.17 mm
	1000 rpm	4.40 mm

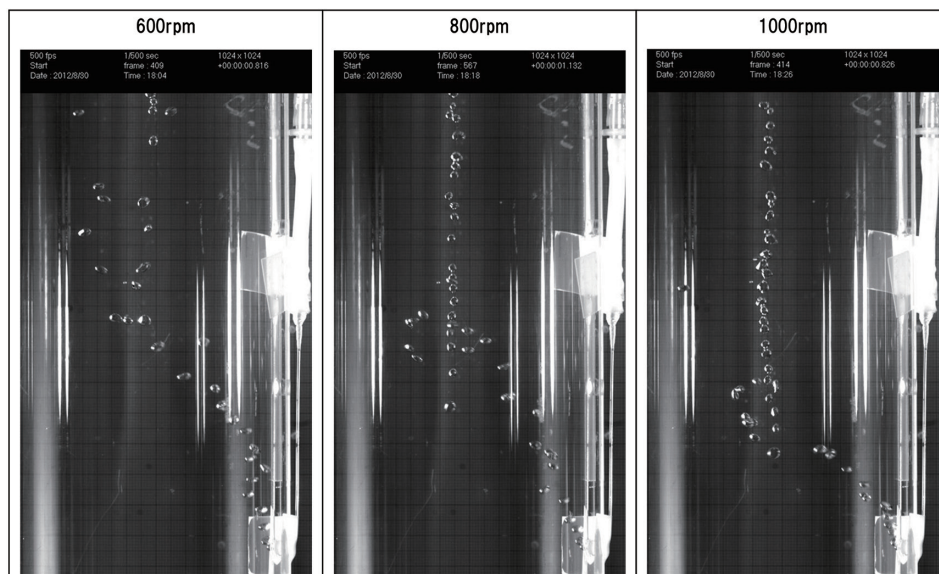


Fig. 11 High speed camera images of bubbles blown in swirl flow

Sutherland established for a potential flow and the model that Weber and Paddock established for a transitional flow region. The experimental values are higher than the values obtained using the model assuming a rigid bubble surface and the model for a Stokes flow.

The particle capture efficiency is expressed by Equation (7), in general. The coefficients A and n are classified as shown in Fig. 13<sup>2-4)</sup> depending on the intensity of the flow (Reynolds number for bubbles) and the surface state of the bubbles (mobile or rigid). Figure 13 shows the representative model in each region.

$$E = A \left( \frac{d_p}{d_b} \right)^n \quad (7)$$

The reason why the particle capture efficiency does not reach 100% is that, as schematically shown in Fig. 10, particles following the flows around the bubbles avoid the traveling bubbles. The comparison of the models shown in Fig. 13 indicates that when the bubbles are smaller compared with the particles and when the flow is intense (a potential flow, not a Stokes flow) and the surface of the bubbles easily deform, the capture efficiency improves.

Conditions of particles capture efficiency of 1% indicated in Fig. 12 are that, when the particle diameter is 10 μm, the bubble diameter needs to be 3 mm; and when the particle diameter is 50 μm, the bubble diameter needs to be 15 mm. Under these conditions, when 100 bubbles sweep a region where one particle exists, the particle will be perfectly removed. On the contrary, when the bubble diameter is one tenth (1/10) of the aforementioned conditions (when the

particle diameter is 10 μm, the bubble diameter is 0.3 mm or when the particle diameter is 50 μm, the bubble diameter is 1.5 mm), the capture efficiency increases to 10%.

Thus, bubbles can remove only particles with relatively large diameters compared to their own diameters. What is required to remove inclusions in molten steel effectively is to generate very small bubbles or processes, in which small particles are coalesced and removed by bubbles simultaneously. Some consider that it is acceptable to remove only large harmful inclusions. However, inclusions easily condense (e.g., alumina) and become larger in the subsequent processes. Therefore, inclusions that are considerably smaller than inclusions that are regarded as harmful must be removed in upstream manufacturing processes. Otherwise, the processes to remove inclusions are not effective.

**2.6 Summary of experimental results**

The speed at which a bubble removes particles (particle removal rate constant  $k_g$ ) can be calculated by Equation (8) when following the Sutherland's model and by Equation (9) when following the Weber and Paddock's model. When an bubble receiving centripetal force in the swirl flow moves in the radial direction at a relatively high speed similar to the floating terminal velocity (Reynolds number for bubbles ≈ 800 to 1000) like the conditions in this experiment, the calculation results of the two models are approximately equal as shown in Fig. 12.

$$\frac{dC_p}{dt} = k_g C_p = \frac{\pi(d_p+d_b)^2}{4} u_b \cdot 3 \cdot \left( \frac{d_p}{d_b} \right) \cdot C_b \cdot C_p \quad (8)$$

$$\frac{dC_p}{dt} = k_g C_p = \frac{\pi(d_p+d_b)^2}{4} u_b \cdot \left[ 1 + \frac{2}{1+(37/Re_b)^{0.85}} \right] \cdot \left( \frac{d_p}{d_b} \right) \cdot C_b \cdot C_p \quad (9)$$

The Reynolds number for bubbles,  $Re_b$ , is defined by Equation (10).

$$Re_b = \frac{u_b d_b \rho}{\mu} \quad (10)$$

Where,  $C_p$  is the number concentration of particles,  $\rho$  is the difference in the density between the bubble and liquid, and  $\mu$  is the viscosity of the liquid.

**3. Conclusions**

The purpose of this study was to clarify the mechanism of inclusion removal by bubbles in molten steel. The particle capturing efficiency was calculated by the water model experimental data in which bubbles were blown into the swirl flow. The results indicate that wettable particles are not captured (they do not attach to bubbles) and non-wettable particles are captured at a rate constant equal

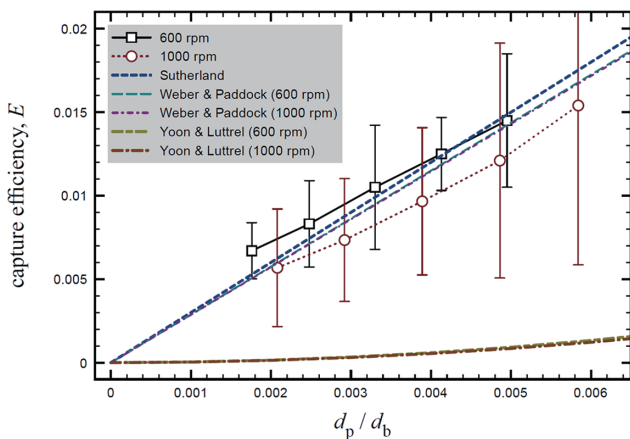
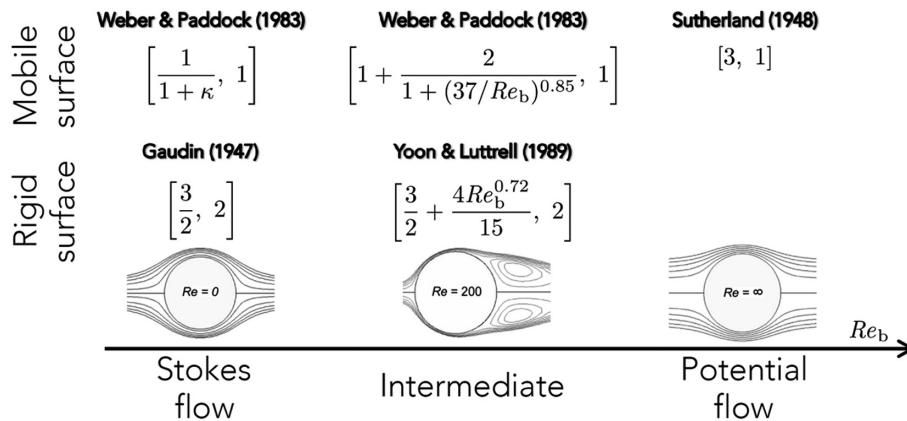


Fig. 12 Capture efficiency in swirl flow region



Illustrations of streamline are quoted from Int. J. Miner. Process. 239, 72 (2003) by Phan, C.M. et al.

Fig. 13 Popular models of particle capture efficiency<sup>2-4)</sup> ([A, n] in Equation (7))

to that in the Sutherland's model or Weber and Paddock's model. The experimental results show that it is important in actual manufacturing processes to generate fine bubbles and consolidate inclusions simultaneously to enhance the efficiency of inclusion removal by bubbles.

The obtained particle capturing efficiency of a single bubble is at the highest level among the values estimated using various existing models. Nippon Steel is experimentally analyzing at present whether these experimental results obtained for swirl flows can be applied to a single bubble that floats to the surface in a static bath. In addition, we are working to clarify the entire mechanism to remove inclusions in molten steel by studying the particle transfer mechanism with congregated bubbles. In addition, Nippon Steel is working to develop inclusion removal processes that are deductively derived from a series of research results and apply them to the actual equipment, aiming at acute purification of molten steel.

#### Acknowledgments

This paper is a summary of results of the cooperative study with Tohoku University. I express my gratitude to Prof. Shoji Taniguchi, a current emeritus professor at Tohoku University, who gave me careful but strict instructions. I performed experiments with Prof. Shinichi Shimasaki, an associate professor at the National Institute of Technology, Kagawa College and I was allowed to participate in the discussion for organizing data, which enabled me to learn many things. I extend my deep gratitude to them.

#### References

- 1) Hinze, J.O.: Turbulence. New York, McGraw-Hill, 1975
- 2) Sutherland, K.L.: Physical Chemistry of Flotation. XI. Kinetics of the Flotation Process. *J. Phys. Chem.* 52, 394–425 (1948)
- 3) Weber, M.E., Paddock, D.: Interceptional and Gravitational Collision Efficiencies for Single Collectors at Intermediate Reynolds Numbers. *J. Colloid Interface Sci.* 94, 328–335 (1983)
- 4) Yoon, R.H., Luttrell, G.H.: The Effect of Bubble Size on Fine Particle Flotation. *Min. Proc. Extract. Metall. Rev.* 5, 101–122 (1989)



Yuichi TSUKAGUCHI  
Senior Researcher, Ph. D.  
Steelmaking Research Lab.  
Process Research Laboratories  
16-1 Sunayama, Kamisu City, Ibaraki Pref. 314-0255